Chemistry–A European Journal
Concept
doi.org/10.1002/chem.202200479
Chemistry Europe
European Chemical Societies Publishing
www.chemeurj.org

Renaissance of Topotactic Ion-Exchange for Functional Solids with Close Packed Structures

Eric Gabilondo,[a] Shaun O'Donnell,[a] Ryan Newell,[b] Rachel Broughton,[b] Marcelo Mateus,[b] Jacob L. Jones,[b] and Paul A. Maggard*[a]

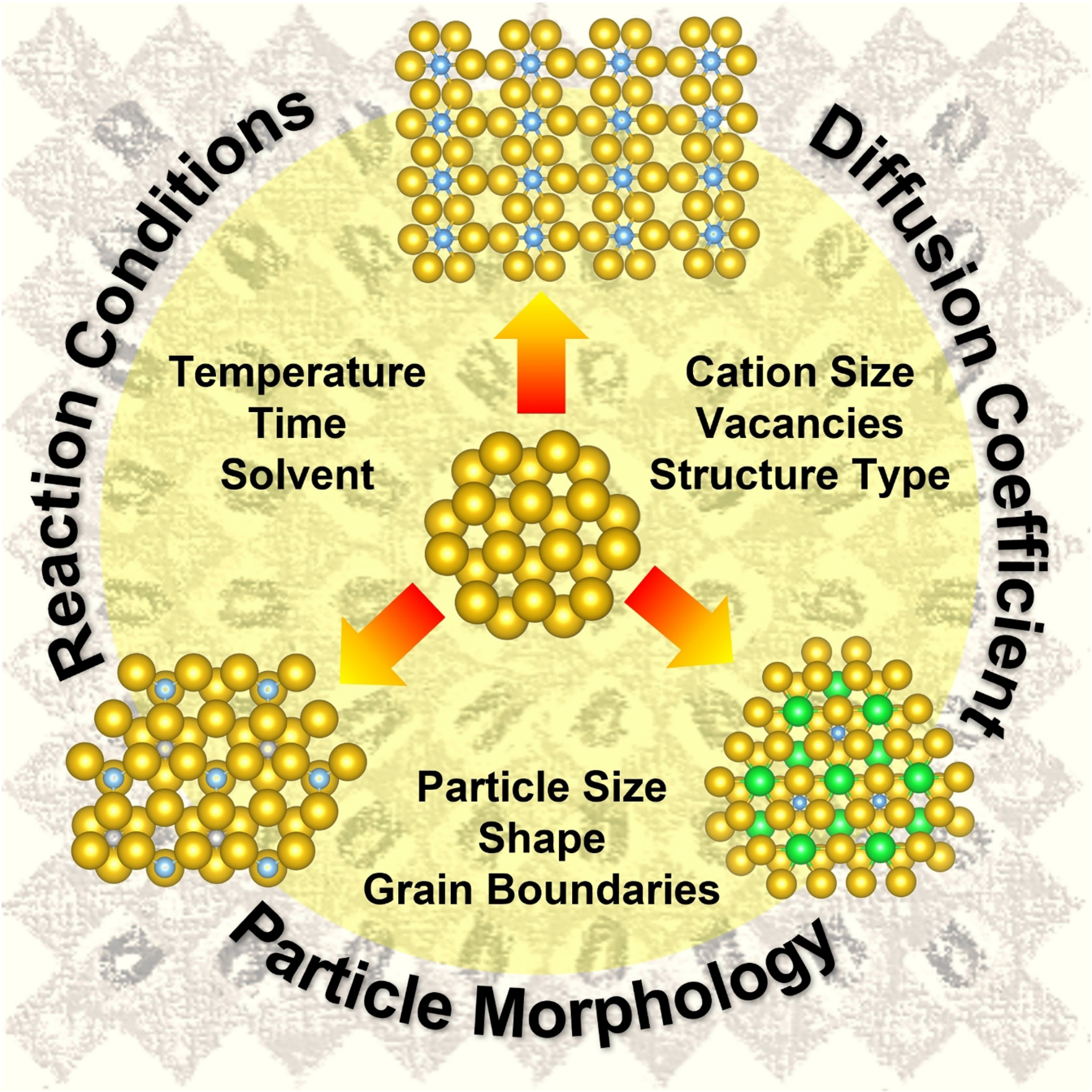

Abstract: Recently, many new, complex, functional oxides have been discovered with the surprising use of topotactic ion-exchange reactions on close-packed structures, such as found for wurtzite, rutile, perovskite, and other structure types. Despite a lack of apparent cation-diffusion pathways in these structure types, synthetic low-temperature transformations are possible with the interdiffusion and exchange of functional cations possessing ns^2 stereoactive lone pairs (e.g., Sn(II)) or unpaired nd^x electrons (e.g., Co(II)), targeting new and favorable modulations of their electronic, magnetic, or catalytic properties. This enables a synergistic blending of new functionality to an underlying three-dimensional connectivity, i.e., $[\text{-M–O-M-O-}]_n$, that is maintained during the transformation. In many cases, this tactic represents the only known pathway to prepare thermodynamically unstable solids that otherwise would commonly decompose by phase segregation, such as that recently applied to the discovery of many new small bandgap semiconductors.

Introduction

Historically, topotactic ion-exchange reactions have been a foundational component in the development of functional solids for many key technologies, including for the preparation of functional batteries, supercapacitors, fuel cells or zeolites to name a few.[1,2] Facile ion exchange in these types of materials is well established as arising within crystalline structures exhibiting the capacity for high ion-mobility. For example, this typically occurs between the layers or through the pore openings that are found in layered or porous crystalline structures.[3–5] Additionally, thermodynamically unstable compounds, i.e., metastable compounds, can frequently be synthesized via maintenance of the underlying crystalline structure during the ion-exchange reaction.[6–8] Thus, low-temperature ion-exchange reactions provide a valuable kinetic handle for the formation of new, and frequently metastable, crystalline solids.

Until recently, however, the advantages of ion-exchange reactions have remained significantly less explored for close-packed structures, such as for those in the highly common wurtzite, rutile, or spinel structure types shown in Figure 1. Their three-dimensional connectivity, $[\text{-M–O-M-O-}]_n$, is advantageous for achieving a high carrier mobility, long-range magnetic ordering and many other properties. The tantalizing possibility of literally thousands of undiscovered solids having these structure types has been predicted by high-throughput computational studies.[9–11] One main reason that cation-exchange routes have remained predominantly unrealized is that these structure types appear, by most sensible arguments, to unfortunately restrict the possibility of any significant ion interdiffusion at low temperatures. Only recently has this notion been proven demonstrably false by the budding renaissance of research into cation exchange within solids having three-dimensional close-packed structures. The aim of this paper is to elucidate the emerging concepts underlying successful reaction tactics that are aimed at attaining new crystalline solids for investigation of their physical properties.

Cation Exchange in Close-Packed Structures

An initial question to pose is under what conditions would close-packed solids be capable of exhibiting ion exchange? Assuming an excess of exchangeable cations and concentration gradient ($\partial C/\partial x$), according to kinetic exchange theory the rate determining step is chemical diffusion within the solid, with the fraction (f) of cation exchange at equilibrium being a function of particle radius (r), chemical diffusion coefficient (D_c), and time (t) as derived:[1,12,13] $f = 1\text{-}(6/\pi^2)\Sigma[\exp(\text{-}n^2Bt)]/n^2$ (1), and $B = \pi^2 D_c/r^2$ and $n = 1$ to ∞. This percentage represents the extent of reaching the maximum attainable cation exchange as deter-

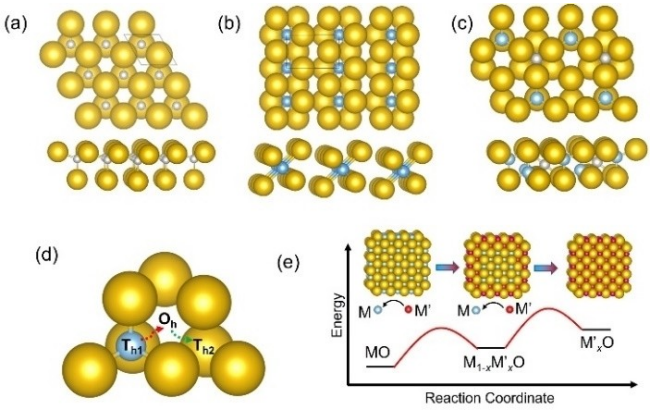

Figure 1. Structural views of close packed anions (yellow) with cations (blue/gray): shows filling the (a) tetrahedral sites to give a zinc blend or wurtzite type layer, (b) half of the octahedral sites to give a rutile type layer, and (c) a fraction of the tetrahedral and octahedral sites to give a spinel type layer; (d) a diffusion pathway of a tetrahedral cation and the (e) surface cation-exchange leading to a metastable solid.

[a] *E. Gabilondo, S. O'Donnell, Dr. P. A. Maggard*
Department of Chemistry
North Carolina State University
Raleigh, NC 27695 (USA)
E-mail: paul_maggard@ncsu.edu

[b] *Dr. R. Newell, R. Broughton, M. Mateus, Dr. J. L. Jones*
Department of Materials Science and Engineering
North Carolina State University
Raleigh, NC 27695 (USA)

Supporting information for this article is available on the WWW under https://doi.org/10.1002/chem.202200479

Selected by the Editorial Office for our Showcase of outstanding Review-type articles (www.chemeurj.org/showcase).

mined by thermodynamics, which may be some fraction of full exchange. Illustrated in Figure 2, for even small chemical diffusion constants (D_c) of ~10^{-15} cm^2 s^{-1}, nearly complete cation exchange (95%) is attainable on the order of about 4 weeks for even surprisingly large 100 μm particles. For crystallite sizes in the nanoscale range of ~20 to 40 nm in diameter, equilibrium can be reached within a few days for a D_c even as small as 10^{-19} cm^2 s^{-1}. Whether a solid exhibits a sufficient D_c at the low reaction temperatures of 500–800 K depends on its composition and structure.

Many binary metal chalcogenides easily satisfy these conditions, with a relatively large D_c in the low temperature range of ~400-700 K of ~10^{-8} to 10^{-7} cm^2 s^{-1} (FeS, MnS, NiS) and up to as large as ~10^{-6} to 10^{-5} (α-Ag_2S and Cu_2S).[14,15] Hence, metal chalcogenides have been intensely investigated in low-temperature, solution-based exchange reactions in a growing number of recent studies,[16–19] such as starting from Cu_2S with a distorted antifluorite structure. This has yielded unique synthetic access to metastable polymorphs of binary chalcogenides, yielding the metastable CoS and MnS in either the wurtzite type or zinc-blende type structures.[16,17] Starting from the metal-oleylamine complexes, these exchange reactions occur rapidly and topotactically in trioctylphosphine at only 373 to 473 K with the maintenance of the underlying close-packed structure, for example, $Cu_{2-x}S$ (hcp)→CoS (hcp) for the wurtzite structure, and kinetically stabilizing new metastable polymorphs. By comparison, metal oxides exhibit D_c values up to an order of magnitude smaller (or less) than metal sulfides.[14,15] Nonetheless, the solution-based cation exchange of Fe(II) for Co(II) cations at the particles' surfaces at only ~500 K has recently been used to prepare core-shell FeO/$CoFe_2O_4$ particles with the inverse spinel structure type.[20] Of note, these particles were found to show enhanced magnetic remanence, coercivity, as well as superparamagnetic blocking temperature as compared to homogeneous magnetite.

Recent research has made clear the successful synthetic approaches possible via the low-temperature cation exchange of close-packed structures, despite having very small chemical diffusion coefficients. The maintenance of their underlying anion sublattice, whether it be hexagonal or cubic close-packed, has enabled the study of a growing number of new binary compounds and a renaissance of research activity that had previously been considered as unpractical using this synthetic approach.

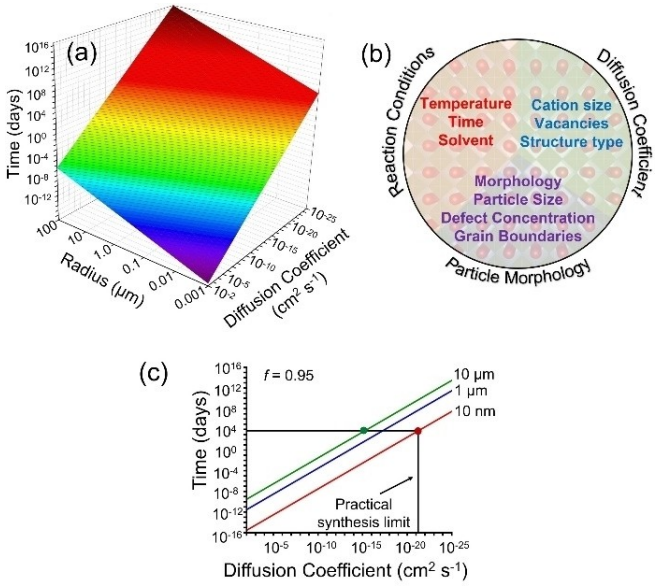

Figure 2. (a) Plot of reaching 95% cation exchange with reaction time, particle radius, and chemical diffusion coefficient, (b) the tunable synthetic handles, and (c) the calculated reaction time versus diffusion coefficient for different particle radii.

Cation Exchange in the Preparation of Functional Multinary Oxides

Topotactic cation exchange of close-packed structures has also recently proven productive in the synthesis of many new, complex, multinary oxides, i.e., M'MO_x. The basic strategy has involved the maintenance of not only the anion sublattice, but the preservation of the underlying [-M–O-M-O-]$_n$ connectivity during the exchange of a secondary metal cation (M'). This enables the addition of new functionality to an existing [-M–O-M-O-]$_n$ framework, such as for the visible-light sensitization of existing structures by the incorporation of Cu(I), Ag(I), Fe(II) or Sn(II) cations. Described below, many small bandgap semiconductors have been discovered by this approach starting from close-packed structures having the wurtzite, rutile, pyrochlore and perovskite type structures.

Replacement of a single type of metal cation (M') in a M'MO_x solid relies upon its selective diffusion through the 'MO_x'-based network, as found for many types of transition-metal oxides containing alkali and alkaline earth cations. For example, new visible-light photocatalysts have been synthesized with wurtzite-type structures,[21,22] as given in the reactions below:

$$\beta\text{-}NaGaO_2 + CuCl \rightarrow \beta\text{-}CuGaO_2 + NaCl \quad (1)$$

(wurtzite type)

$$Na_2ZnGeO_4 + 2CuCl \rightarrow Cu_2ZnGeO_4 + 2NaCl \quad (2)$$

(double wurtzite type)

Thermodynamically, these reactions are driven by the co-formation of the highly stable NaCl salt. Kinetically, the sodium cations diffuse through the close-packed structure, Figure 1, within micrometer-sized particles to exchange at the surfaces with the Cu(I) cations of the molten CuCl at only 425 to 525 K. This approach maintains the underlying 'GaO_2' or '$ZnGeO_4$' lattices while the cation substitution occurs within the tetrahedral cavities containing the Na cation, Figure 1a. Both β-$CuGaO_2$ and Cu_2ZnGeO_4 exhibit highly dispersed conduction bands and have favorably low electron effective masses of ~0.2 m_e^*/m_0. After a topotactic exchange of Cu(I) cations that provides a higher energy valence band, each exhibits a small, direct

bandgap (~1.4 – 1.5 eV). This added feature addresses the need for incorporating the strong, broad-wavelength absorption of sunlight together with a low effective electron mass. Similar examples of Ag(I) cation exchange have been reported for related structure types as well.[23,24]

The topotactic exchange of Fe(II) cations has also been demonstrated in the triple-rutile structure for $LiMWO_6$ (M = Nb or Sb), a reported Li-ionic conductor.[25] The exchangeable Li cations are coordinated within its octahedral sites. For large, micrometer-sized particles, a nearly complete cation exchange with Fe(II) cations in a 0.2 M aqueous solution occurs at only 333 K of up to ~90-92%, or $Li_{1-x}Fe_{x/2}MWO_6$ ($x = 0.9$ to 0.92; 2:1 ratio of Li:Fe).[26,27] The 'MWO_6' networks, having buckled close-packed layers, are preserved with the incorporation of Fe(II) cations over 25% of the octahedral sites. The thermodynamic driving force of the reaction has yet to be explored, as both solids are metastable. There is a significant redshift of the band gap from ~3.0 eV down to ~1.71 eV or ~2.06 eV, for M = Nb and Sb respectively. The Fe(II) cations occur in a high spin, $3d^6$, configuration with an antiferromagnetic transition occurring at ~20 K. In photocatalytic tests, the latter shows visible-light activity for the degradation of rhodamine blue.

The most intensely investigated topotactic exchange reactions within close-packed structures have perhaps involved the Sn(II) cation using an aqueous solution or one of its halide-salt fluxes. A common motivation is to prepare visible-light, semiconducting photocatalysts with a higher energy valence band formed by the Sn(II) cation. These have involved metal oxides in the pyrochlore[28–30] and other structure types.[31–34] The Maggard and Jones groups have pioneered recent studies of Sn(II) exchange into the perovskite structure type, $BaMO_3$ (M = Ti, Zr, or Hf) with close-packed 'BaO_3' layers, as illustrated in Figure 3 and in the reactions below:

$$BaHfO_3 + x\ SnClF \rightarrow (Ba_{1-x}Sn_x)HfO_3 + x\ BaClF \quad (3)$$

$$BaZr_{1/2}Ti_{1/2}O_3 + x\ SnClF \rightarrow (Ba_{1-x}Sn_x)Zr_{1/2}Ti_{1/2}O_3 + x\ BaClF \quad (4)$$

In a novel twist, the exchangeable Ba cations occupy sites within the close-packed layers (rather than within the tetrahedral or octahedral cavities), while the 'MO_3' sublattice remains preserved. The formation of the stable BaClF salt drives the overall reaction to form the highly metastable Sn(II) perovskites, containing from ~50% to 100% Sn(II) cations on the A-sites.

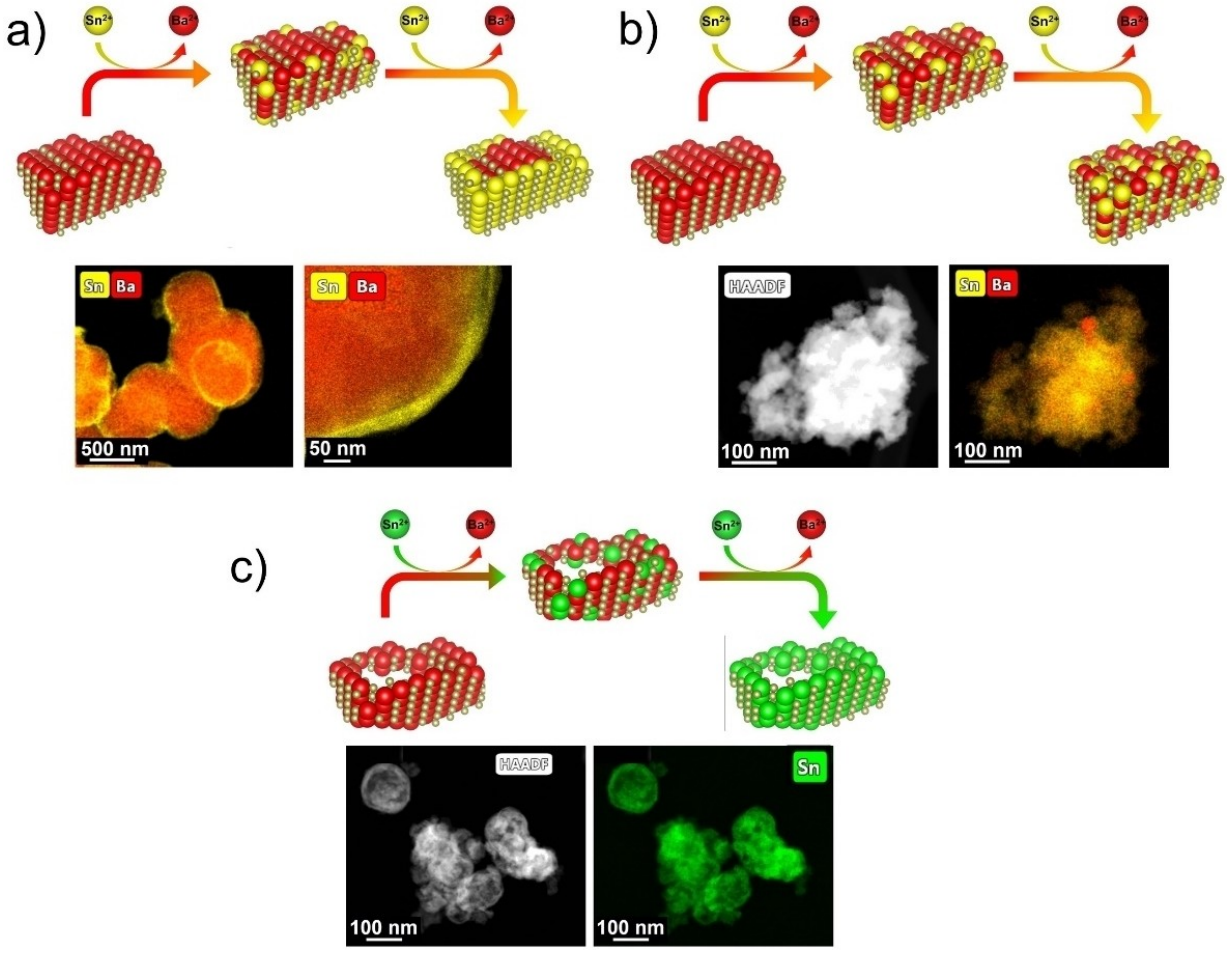

Figure 3. Toptactic exchange of Sn(II) cations into $BaMO_3$ perovskites, yielding (a) shell-core $SnZr_{1/2}Ti_{1/2}O_3$-$BaZr_{1/2}Ti_{1/2}O_3$, (b) large particles of Sn(II)-mixed $Ba_{1-x}Sn_xHfO_3$ and (c) nano-eggshells of pure $SnHfO_3$, with insets of TEM/EDS images.

This leads to both a smaller bandgap of down to ~1.95 eV and visible-light photocatalytic activity for the production of molecular oxygen.[33]

Prior studies have shown chemical diffusion constants of Ba cations in the perovskite structure on the order of 10^{-18} to 10^{-20} cm^2 s^{-1} at 1200 K,[35] i.e., falling at the outer edges of the practical synthesis limits in Figure 2. In general, reaction diffusion coefficients for solids are usually higher by up to 3 or 6 orders of magnitude compared to self-diffusion coefficients.[36] As expected, the homogeneity and extent of Sn(II)-diffusion show a sensitive dependence on the particle sizes/morphology and chemical composition. Topotactic Sn(II)-exchange on highly-faceted and smooth particles typically results in thin ~30 to 80 nm shells, as shown for the $SnZr_{1/2}Ti_{1/2}O_3$-$BaZr_{1/2}Ti_{1/2}O_3$ shell-core particles in Figure 3a. More homogeneous distributions of the Sn(II) cation can be achieved by reactions with particles having rough edges, Figure 3b, likely owing to presence of grain boundaries and cracks that facilitate greater cation interdiffusion and exchange. Alternatively, a reduction of the particle sizes down to ~50 to 100 nm can also be effective strategy, as shown for the nano-eggshell morphologies in Figure 3c. These hollow particles consist of thin shells that have been used to shorten the diffusion lengths necessary to attain high purity $SnHfO_3$. The latter is currently under investigation. In prior related research, the topotactic exchange of Ni(II) cations into the perovskite-type $NaTaO_3$ has also been reported using flux reaction conditions, yielding the new $Ni_{0.5}TaO_3$.[37] Experimental evidence is clear that future research into topotactic cation exchange in perovskites will yield a growing abundance of novel, functional oxides.

Summary and Outlook

The rising use of topotactic exchange reactions on close-packed structures holds great promise to enable the preparation of a large range of new multinary solids. The choice of solvent/flux is system specific and is targeted to provide a high cation mobility at low temperatures while also not dissolving or otherwise transforming the sublattice. The advantage of this approach is the capability of maintaining either the underlying a) anion substructure or b) a metal-anion 'MO_x' substructure, while incorporating new functional cations (M') into the framework. Traditional synthetic methods which rely upon full anion/cation diffusion are insufficient to provide this type of kinetic control, and especially so for metastable solids that would rapidly decompose. While the achievement of kinetic control over the formation of three-dimensional structures has long been a grand challenge in crystalline solids, there remain many key challenges and opportunities in the future development of this synthetic approach. For example, chemical diffusion coefficients are known in relatively few systems, hindering a predictability of the synthetic exchangeability of particular cations. In addition, the compatibility of two cations being exchanged for each other will need to be more deeply understood as a function of their differences in cation sizes and preferred coordination environments. For example, while most synthetic reports involve the exchange of isovalent cations, for example, monovalent Cu for Na cations, the synthetic limitations are not yet well understood. Many answers to these challenging problems will be supplied by the topotactic synthetic investigations currently surging in new investigations and being developed for a wide range of potential applications.

Acknowledgements

The authors acknowledge support of this work by National Science Foundation (Grant#: DMR-2004455).

Conflict of Interest

The authors declare no conflict of interest.

Data Availability Statement

Data sharing is not applicable to this article as no new data were created or analyzed in this study.

Keywords: cation exchange · metastability · topotactic reaction · metal oxides · solar energy conversion

[1] W. A. England, J. B. Goodenough, P. J. Wiseman, *J. Solid State Chem.* **1983**, *49*, 289–299.
[2] J. Gopalakrishnan, *Chem. Mater.* **1995**, *7*, 1265–1275.
[3] R. Uppuluri, A. S. Gupta, A. S. Rosas, T. E. Mallouk, *Chem. Soc. Rev.* **2018**, *47*, 2401–2430.
[4] D. L. M. Cordova, D. C. Johnson, *ChemPhysChem* **2020**, *21*, 1345–1368.
[5] M. A. Hayward, *Semicond. Sci. Technol.* **2014**, *29*, 064010(1-8).
[6] A. Parija, G. R. Waetzig, J. L. Andrews, S. Banerjee, *J. Phys. Chem. C* **2018**, *122*, 25709–25728.
[7] J. R. Chamorro, T. M. McQueen, *Acc. Chem. Res.* **2018**, *51*, 2918–2925.
[8] P. A. Maggard, *Acc. Chem. Res.* **2021**, *54*, 3160–3171.
[9] C. J. Bartel, C. Sutton, B. R. Goldsmith, R. Ouyang, C. B. Musgrave, L. M. Ghiringhelli, M. Scheffler, *Sci. Adv.* **2019**, *5*, eaav0693(1-9).
[10] M. R. Filip, F. Giustino, *Proc. Nat. Acad. Sci.* **2018**, *115*, 5397–5402.
[11] J. Koettgen, C. J. Bartel, G. Ceder, *Chem. Commun.* **2020**, *56*, 1952–1955.
[12] W. C. Bauman, J. Eichhorn, *J. Am. Chem. Soc.* **1947**, *69*, 2830–2836.
[13] D. Reichenberg, *J. Am. Chem. Soc.* **1953**, *75*, 589–597.
[14] S. Mrowec, K. Przybylski, *High Temp. Mater. Processes* **1984**, *6*, 1–79.
[15] J. A. Van Orman, K. L. Crispin, *Rev. Mineral. Geochem.* **2010**, *72*, 757–825.
[16] A. E. Powell, J. M. Hodges, R. E. Schaak, *J. Am. Chem. Soc.* **2016**, *138*, 471–474.
[17] J. L. Fenton, R. E. Schaak, *Angew. Chem. Int. Ed.* **2017**, *56*, 6464–6467; *Angew. Chem.* **2017**, *129*, 6564–6567.
[18] G. Gariano, V. Lesnyak, R. Brescia, G. Bertoni, Z. Dang, R. Gaspari, L. De Trizio, L. Manna, *J. Am. Chem. Soc.* **2017**, *139*, 9583–9590.
[19] M. Saruyama, R. Sato, T. Teranishi, *Acc. Chem. Res.* **2021**, *54*, 765–775.
[20] M. Sytnyk, R. Kirchschlager, M. I. Bodnarchuk, D. Primetzhofer, D. Kriegner, H. Enser, J. Stangl, P. Bauer, M. Voith, A. W. Hassel, F. Krumeich, F. Ludwig, A. Meingast, G. Kothleitner, M. V. Kovalenko, W. Heiss, *Nano Lett.* **2013**, *13*, 586–593.
[21] T. Omata, H. Nagatani, I. Suzuki, M. Kita, H. Yanagi, N. Ohashi, *J. Am. Chem. Soc.* **2014**, *136*, 3378–3381.
[22] M. Kita, I. Suzuki, N. Ohashi, T. Omata, *Inorg. Chem.* **2017**, *56*, 14277–14283.
[23] D. Arney, P. A. Maggard, *ACS Catal.* **2012**, *2*, 1711–1717.
[24] J. Boltersdorf, T. Wong, P. A. Maggard, *ACS Catal.* **2013**, *3*, 2943–2953.
[25] H. Ohtsuka, A. Yamaji, T. Okada, *Sol. St. Ion.* **1984**, *14*, 283–288.

[26] V. Meena, J. Malik, T. K. Mandal, *ACS Appl. Electron. Mater.* **2021**, *3*, 2504–2511.
[27] V. Meena, T. K. Mandal, *Inorg. Chem.* **2019**, *58*, 2921–2924.
[28] S. Uma, J. Singh, V. Thakral, *Inorg. Chem.* **2009**, *48*, 11624–11630.
[29] M. Weiss, T. Bredow, R. Marschall, *Chem. Eur. J.* **2018**, *24*, 18535–18543.
[30] M. Weiss, R. Marschall, *Nanoscale* **2018**, *10*, 9691–9697.
[31] J. Boltersdorf, B. Zoellner, C. Fancher, J. L. Jones, P. A. Maggard, *J. Phys. Chem. C* **2016**, *120*, 19175–19188.
[32] Y. Zou, J. Le, Y. Cao, N. An, Y. Zhou, J. Li, D. Liu, Y. Kuang, *J. Mater. Chem. A* **2021**, *9*, 20185–21093.
[33] S. C. O'Donnell, C.-C. Chung, A. Carbone, R. Broughton, J. L. Jones, P. A. Maggard, *Chem. Mater.* **2020**, *32*, 3054–3064.
[34] E. A. Gabilondo, S. C. O'Donnell, R. Broughton, J. L. Jones, P. A. Maggard, *J. Solid State Chem.* **2021**, *302*, 122419(1-10).
[35] M. F. Kessel, *Anion and Cation Diffusion in Barium and Strontium Titanate*, Ph.D. Thesis (Aachen, 2012).
[36] V. I. Dybkov, Reaction Diffusion and Solid State Chemical Kinetics, Trans Tech Publications: Zurich, Switzerland (2010).
[37] M. A. Patino, T. Smith, W. Zhang, P. S. Halasyamani, M. A. Hayward, *Inorg. Chem.* **2014**, *53*, 8020–8024.

Manuscript received: February 14, 2022
Accepted manuscript online: April 7, 2022
Version of record online: April 21, 2022